ADVANCED MANUFACTURING TECHNOLOGIES UTILISING HIGH DENSITY INFRARED RADIANT HEATING

J. D. K. Rivard, C. A. Blue, R. D. Ott, A. Sabau, M. Santella, T.-Y. Pan and A. Joaquin

Oak Ridge National Laboratory has developed a unique rapid heating capability utilising a high density infrared (HDI) radiant plasma arc lamp. Power densities $\leqslant 3{\cdot}5$ W cm^{-2} are achievable over an area $35\times 3{\cdot}175$ cm. The power output of the lamp is continuously variable over a range from 1·5% to 100% of available power, and power changes can occur in <20 ms. Processing temperatures $\leqslant 3000^\circ$C can be obtained in a wide variety of processing environments, making HDI a flexible processing tool. Recently, this newly developed heating method was used to investigate selective softening, i.e. hardness reduction of 6063-T6 aluminium alloy. By changing the incident power and exposure time, the percentage reduction in hardness and softened zone size can be varied. It is shown that computer modelling can be used to predict the thermal history and the resulting heat affected zone during HDI processing. In the present work, a 50% reduction in hardness was achieved and confirmed by mechanical testing and microstructural investigation. Micrographs of softened aluminium show that Mg_2Si precipitates had dissolved back into solution. This new approach allows materials to be engineered for a predetermined response to dynamic loading or other environmental situations. SE/S282

Drs Rivard (rivardjd@ornl.gov), Blue, Ott, Sabau and Santella are at the Oak Ridge National Laboratory, Metals and Ceramics Division, Oak Ridge, TN 37831, USA and Drs Pan and Joaquin are at the Ford Research Laboratory, Manufacturing Systems Department, Dearborn, MI 48124, USA. *Manuscript received 5 August 2003; accepted 11 February 2004.*

***Keywords**: High density infrared processing, Plasma arc lamp heating, Preferential heat treating, Aluminium alloys, Radiant heat transfer modelling, Effective processing time, Thermophysical properties*

INTRODUCTION

Vehicle occupant safety is of the utmost concern for the automotive industry. Years of research have led designers to incorporate an impact absorbing body crush zone and a high rigidity cabin, i.e. a zone where deformation and crash energy absorption can occur, while a second zone is maintained in which the passengers are held in a rigid structure where deformation does not occur. Within the zone where deformation occurs, it is necessary to engineer these components to deform at controlled rates during impact. This can be achieved by designing the sectional shape of each framework member and the strength and thickness of each member according to estimated loads at each application. Traditional steel construction allowed for the addition of crimped sections to frame rails for predetermined crash energy absorption. As the frame rails crush, these triggers allow it to collapse on itself in a controlled manner.

With the ever present needs of weight reduction and increasing fuel economy, however, the use of aluminium alloys for frame rail structures is becoming more prevalent. The specific location of the aluminium frame rails is shown in Fig. 1. Extruded aluminium has the benefit of much lower tooling costs compared with stamped aluminium. However, a limitation of extruded aluminium in front rail applications is that the traditional crimped crumple zones used on steel counterparts are impossible to obtain on an extruded tube.

High density infrared (HDI) offers a unique solution to controlling deformation of crumple zones in the event of a crash. By heating an extrusion at periodic intervals with the plasma arc lamp, the material in the heat affected zone shows a significant reduction in hardness and changes in the microstructure. Recent work by Shibata *et al.*[1] demonstrated induction hardening of steel members to increase strength locally in steel body panels. While this method could be applied to aluminium frame rails, HDI holds a critical advantage over induction heating in that HDI processing does not require a rigid apparatus and direct contact for heating, allowing preferential heating of complex shapes.

PLASMA ARC LAMP

The HDI process utilises a unique technology to produce extremely high power densities of 3·5 kW cm^{-2} with a single lamp. Instead of using an electrically heated resistive element to produce radiant energy, controlled and contained plasma is utilised. A schematic of the lamp is shown in Fig. 2.

The lamp consists of a quartz tube 3·175 cm in diameter and 10·16 cm, 20·32 cm or 38·1 cm long. The lamp is sealed at the ends where the cathode and anode are located. Deionised water mixed with argon or nitrogen gas enters at the cathode side through high velocity jets impinging at a given angle. Owing to the high velocities and pressure, the deionised water is impelled to the wall of the quartz tube and spirals down the length of the tube in a uniform film

 DOI 10.1179/026708404225015022

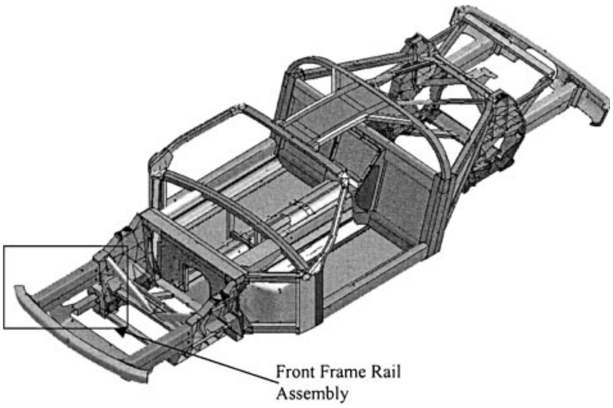

1 *Body structure assemblies showing location of front frame rail assembly, area of interest for replacement of traditional steel construction with extruded aluminium tubes*

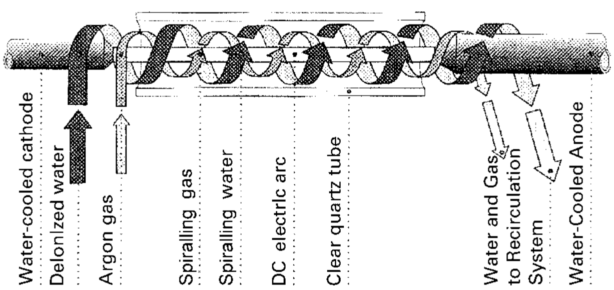

2 *Schematic of high power density lamp and principle operation*

2–3 mm thick. This water film serves two purposes: to cool the quartz wall and to remove any tungsten particulates that may be expelled from the electrodes. The gas moves in a spiral fashion through the centre of the tube, and a capacitative circuit initiates the plasma. The plasma, which has a temperature in excess of 10 000 K, is stable and produces a radiant spectrum 0·2–1·4 μm (Fig. 3).[2]

The spectrum is primarily in the ir (0·78–1·00 μm), although substantial energy is released in the visible wavelength, similar to the appearance of natural sunlight in energy distribution and colour rendition. The spectrum is absorbed with high efficiency by metal surfaces. In contrast, the spectrum of a CO_2 laser with wavelengths near 10·6 μm is absorbed with much lower efficiency.

The lamp has a typical life of approximately 1200 h, and failure occurs in the anode and cathode, which are inexpensive and can be changed in approximately 15 min. Furthermore, the lamp has a

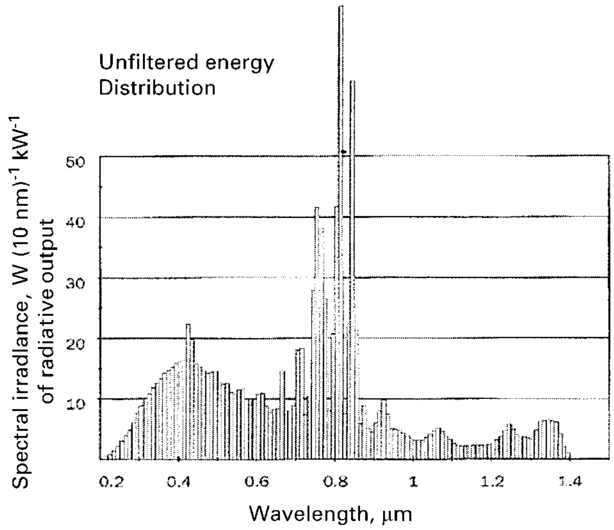

3 *Spectral irradiance produced by plasma arc lamp*

consistent spectral output independent of lamp life and power level. The lamp is typically configured with a reflector to produce a line focus or an area of uniform irradiance (Fig. 4).

The Infrared Processing Center of the Materials Processing Group in the Metals and Ceramics Division at Oak Ridge National Laboratory (ORNL) has a variety of HDI equipment with the capability of producing 10–3500 W cm^{-2} heat fluxes.[3] In the HDI processing facility, the HDI lamp is mounted on a large five axis robotic manipulator arm. A state of the art robotic controller defines arm movement; this controller is capable of using computer aided drawing files of large parts to generate instructions to manipulate the source over a complicated geometry in a predetermined, systematic way. Test sample processing is performed in an environmentally controlled box, which has a quartz window cover to permit processing of materials in a controlled atmosphere. The ir reflector has a focal length which extends through the quartz and onto the material being processed. A lathe for rotating parts during heat treatment is also included in the processing facility.

PROCESS MODELLING

Along with the development of methods for rapidly heat treating materials, a computer model was extended to predict thermal histories as a result of HDI processing or the prediction of appropriate HDI processing parameters. The model was developed within the framework of TELLURIDE,[4] a code

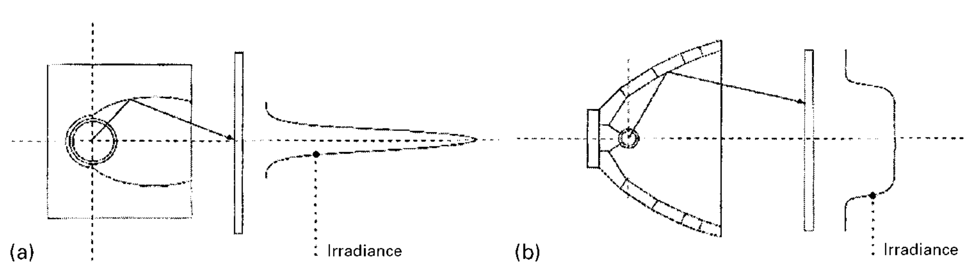

a line focus; *b* uniform irradiance

4 *Typical reflector configurations utilised with high density lamp*

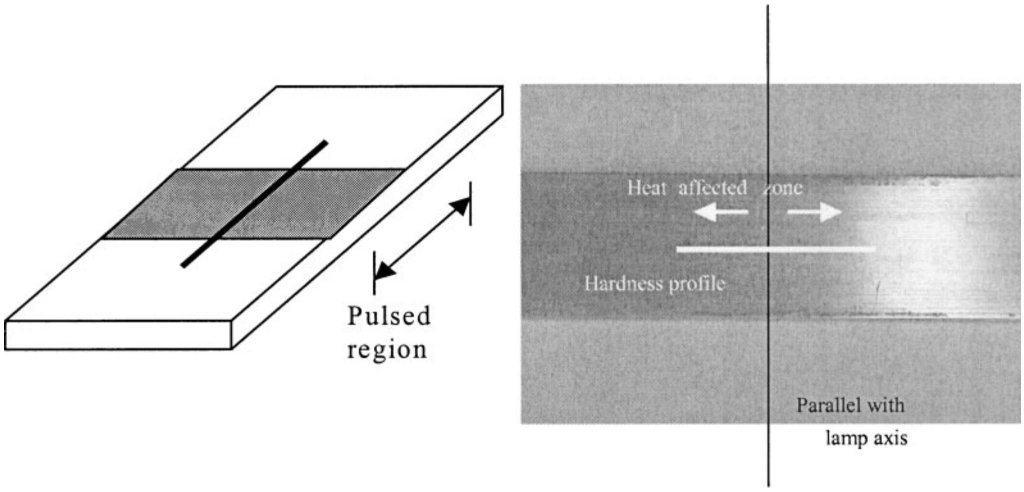

5 *6063-T3 aluminium sample shown with location of lamp, hardness profile and heat affected zone*

developed at Los Alamos National Laboratory for casting simulations. Owing to the modular nature of the code, implementation of the necessary modifications for the modelling of the HDI process was possible.

In performing the heat transfer analysis of the HDI process, the thermophysical properties and process parameters are considered. The thermophysical properties required are emissivity, specific heat, density and thermal conductivity.

The energy equation which describes the heat transfer during HDI processing appears as

$$\frac{\partial \rho h}{\partial t} = \nabla(k\nabla T) \quad (1)$$

where ρ, h, t and T are the density, enthalpy, time and temperature, respectively. The boundary conditions include heat transfer losses due to natural convection and radiation at the surface. At the outer boundaries of the sheet, thermal boundary conditions are imposed such that the heat flux loss is

$$q'' = (h_R + h_c)(T - T_A) \quad (2)$$

where h_R and h_c are the heat transfer coefficients due to radiation and convection with the ambient, respectively. T and T_A are the temperature of the surface and that of the ambient, respectively. For most HDI processing, $h_c = 4{\cdot}18$ W m^{-2} K and

$$h_R = \sigma\varepsilon(T_2 + T_A^2)(T + T_A) \quad (3)$$

where σ is the Stefan–Boltzmann constant, and ε is the emissivity of the surface.

FLAT PLATE PREFERENTIAL SOFTENING

Before undertaking the task of preferentially softening a square tube, a flat plate scenario was investigated to demonstrate the capabilities of the lamp. Samples of 6063-T6 aluminium were machined to 26·0 cm long × 4·7 cm wide × 0·3 cm thick. A thermocouple was spot welded to the back side (side that would be facing away from the lamp) in the centre of the sample. The samples were placed, one at a time, under the lamp in an atmosphere controlled, water cooled processing box. Six samples in total were processed, each one receiving a different lamp exposure. Three samples were exposed to the lamp for 2 s: one at 1·7 kW cm^{-2}, another at 2·0 kW cm^{-2} and a third at 2·4 kW cm^{-2}. The remaining three samples were exposed to the lamp for 8 s, but at lower powers: 0·6 kW cm^{-2}, 0·7 kW cm^{-2} and 0·8 kW cm^{-2}. After processing, each sample had hardness measurements taken as well as a metallographic investigation. Figure 5 shows the sample and the location of the lamp, the range of the heat affected zone and the area in which the hardness profile was measured.

After HDI pulse processing, microhardness testing was performed on each sample. Vickers microhardness was measured on both the lamp exposed pulse side and the back side of each sample. Figure 6 shows the microhardness test results for the samples exposed to 2 s pulses. Figure 7 shows the microhardness test results for the samples exposed to 8 s pulses. All samples exposed to a high energy 2 s pulse show a change in hardness in the heat affected zone. The low power 8 s pulse shows no significant change in hardness in the heat affected zone. The higher power 8 s pulses, however, result in as dramatic a change in hardness as for the 2 s pulses but over a larger area.

Table 1 shows the total energy associated with each pulse. The total energy is calculated by multiplying the power output of the lamp (power density in kilowatts per square centimetre) by the area of the heat affected zone and the pulse duration. Measuring

Table 1 Energy associated with HDI pulse for each sample

Pulse duration, s	Lamp power, kW cm^{-2}	Width, cm	Area, cm^2	kJ
2	1·7	1·7	8·0	27·2
2	2·0	3·6	16·9	67·7
2	2·4	3·5	16·5	77·3
8	0·6	0·75	3·5	16·9
8	0·7	3·9	18·3	102·6
8	0·8	4·6	21·6	138·4

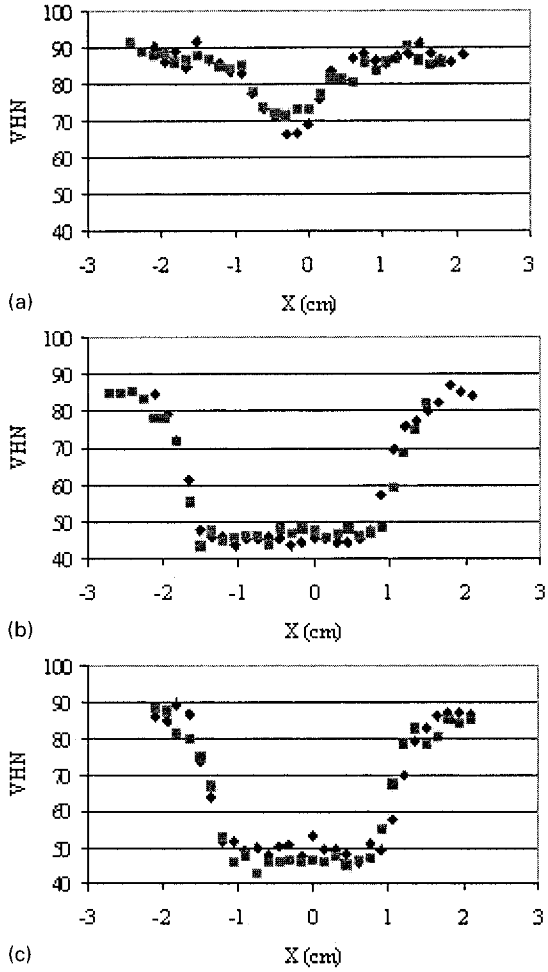

a 1·7 kW cm^{-2}; *b* 2·0 kW cm^{-2}; *c* 2·4 kW cm^{-2}

6 *Results of microhardness testing of 6063-T6 aluminium plates exposed to pulses for 2 s:* ⧫ *pulsed side;* ■ *back side*

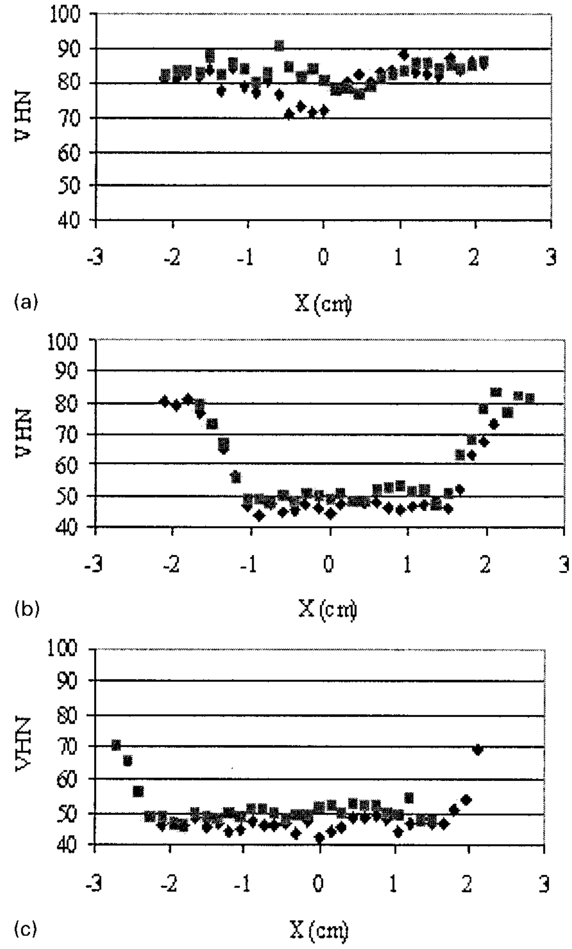

a 0·6 kW cm^{-2}; *b* 0·7 kW cm^{-2}; *c* 0·8 kW cm^{-2}

7 *Results of microhardness testing of 6063-T6 aluminium plates exposed to pulses for 8 s:* ⧫ *pulsed side;* ■ *back side*

the distance over which the hardness values were significantly lower and then multiplying by the width of the sheet determined the heat affected zone.

Using the data from Table 1, Fig. 8 shows the heat affected zone width as a function of the energy input of each pulse. The 0·6 kW cm^{-2}, 8 s pulse had the lowest associated energy and also resulted in the smallest heat affected zone. The 0·8 kW cm^{-2}, 8 s pulse has the highest associated energy and resulted in the largest heat affected zone. Overall, heat affected zone width varied linearly with the associated energy for a given pulse.

The back side temperature was measured during each pulse. Table 2 shows the peak temperatures of the back side of each sample during a given pulse.

Table 2 Back side temperatures during HDI pulse processing

Back side temperature, °C	kJ
295	16·9
309	27·2
405	67·7
407	77·3
401	102·6
399	138·4

The temperatures were plotted versus the amount of energy for each pulse. Again, the 0·6 kW cm^{-2}, 8 s pulse showed the lowest temperature because it received the least amount of energy from the lamp. The 0·8 kW cm^{-2}, 8 s and 1·7 kW cm^{-2}, 2 s pulses showed lower temperatures of ~300°C. All other samples resulted in back side temperatures of ~400°C. Figure 9 shows the temperatures measured as a function of the associated energy. Figure 10 shows the reduction in hardness as a function of associated energy.

Plotting hardness as a function of back side temperature shows that samples that reached a back side temperature of 400°C had hardness values between 40·0 HV and 50·0 HV, and samples that reached a back side temperature of 300°C had hardness values between 70·0 HV and 80·0 HV. Accordingly, a 400°C back side temperature resulted in a 50% reduction in hardness, and a 300°C back side temperature resulted in <30% reduction in hardness. Figure 11 shows the results of the hardness testing as a function of back side temperature.

Micrographs of the 2·4 kW cm^{-2}, 2 s and 0·7 kW cm^{-2}, 8 s pulse samples were taken to investigate the microstructural change due to HDI pulse processing. Figure 12 shows the sectioning of each pulsed sample for microstructural investigation. Micrographs were captured at the surface and along

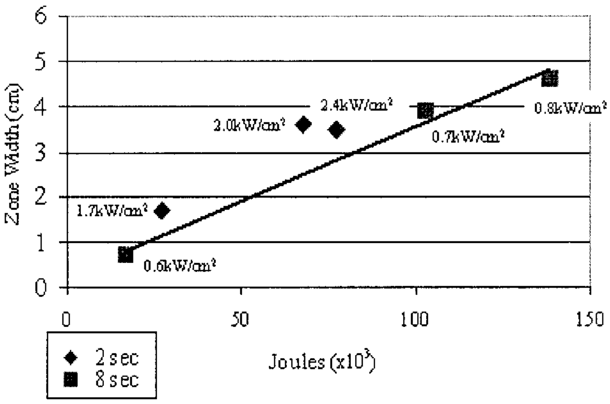

8 *Heat affected zone as function of power associated with pulse*

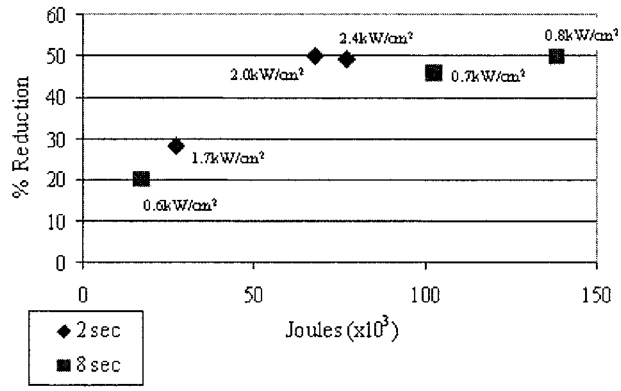

10 *Percentage reduction in hardness as function of associated energy*

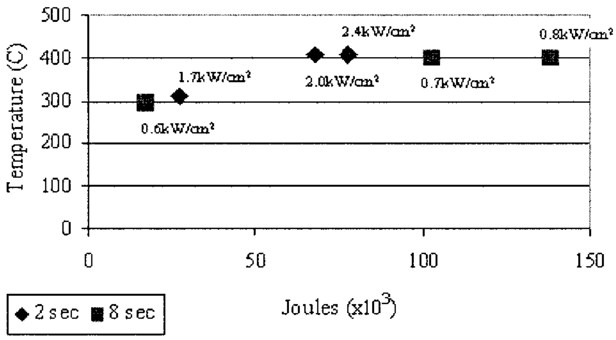

9 *Back side temperature as function of associated energy*

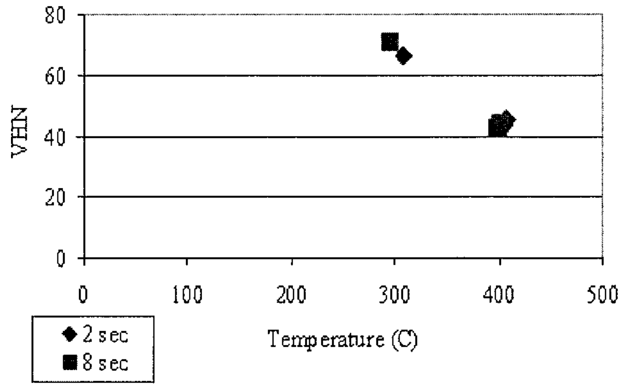

11 *Hardness as function of back side temperature*

the centreline of the sample at four locations: directly under the centreline of the lamp and 1 cm, 2 cm and 3 cm away from the centreline of the lamp. Figure 13 shows the microstructure of the 2·4 kW cm^{-2}, 2 s pulse. Figure 14 shows the microstructure of the 0·7 kW cm^{-2}, 8 s pulse. In both sets of micrographs, Mg_2Si precipitates appear to have dissolved back into solution in the area of the pulse. More precipitates are evident away from the centreline of the lamp. Micrographs from around the centreline of the sample showed a microstructure similar to an overaged condition. That is, the microstructure consisted of a dense precipitate matrix of Mg_2Si and precipitate free zones at the grain boundaries.

MODELLING OF FLAT PLATES

HDI is a highly transient process that can result in a wide range of temperatures over a significant area. Owing to the high thermal conductivity of the aluminium being processed and the resulting heat flow throughout the plate, a model is necessary to predict the annealing effect of processing parameters. The annealing depends on the time–temperature history of the sample. In order to quantify the extent of annealing, an effective processing time (*EPT*) at a reference temperature is defined as follows. *EPT* is based on the time required for self-diffusion to take

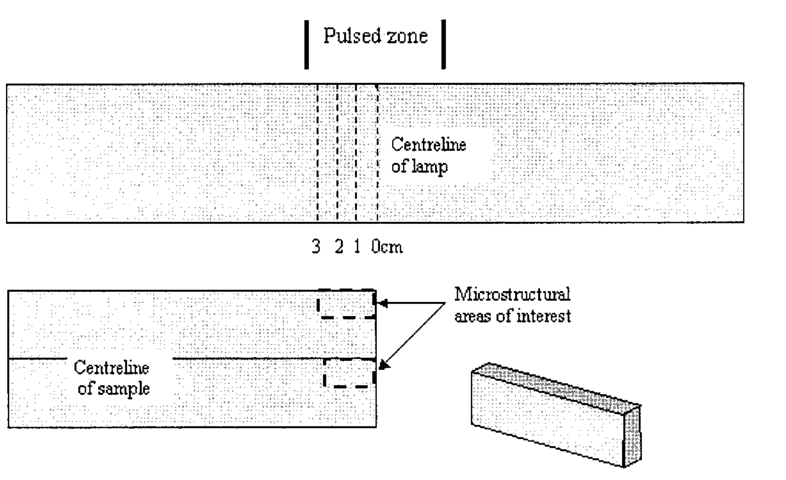

12 *Schematic showing areas in which microstructural changes occurred during HDI pulse processing*

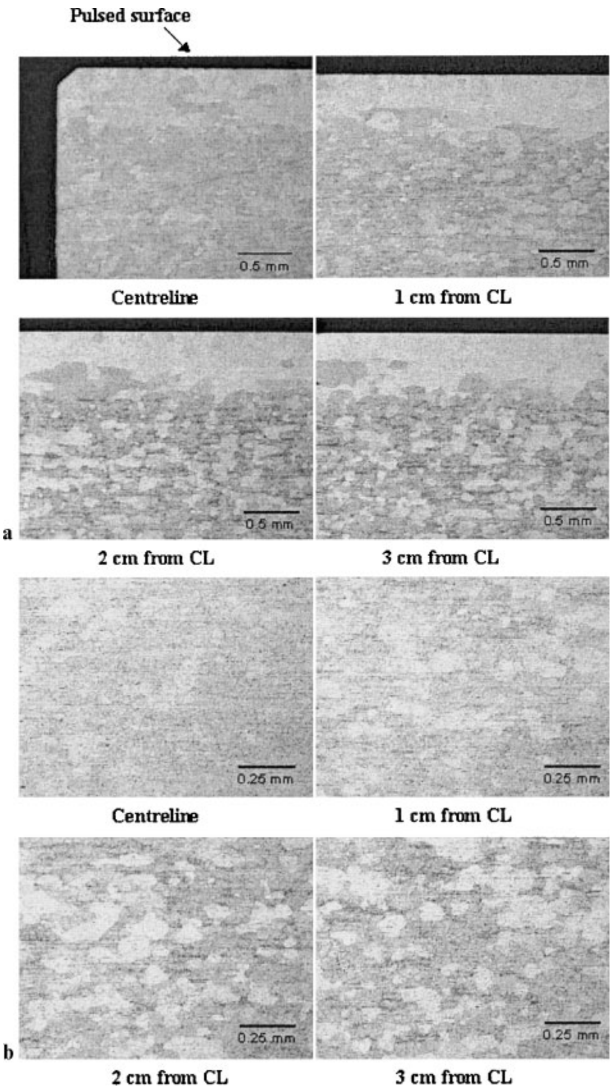

a near surface of sample from directly under centreline of lamp to 3 cm from centreline of lamp; *b* near centreline of sample for same locations

13 *Microstructure of 2·4 kW cm*$^{-2}$*, 2 s pulse aluminium samples*

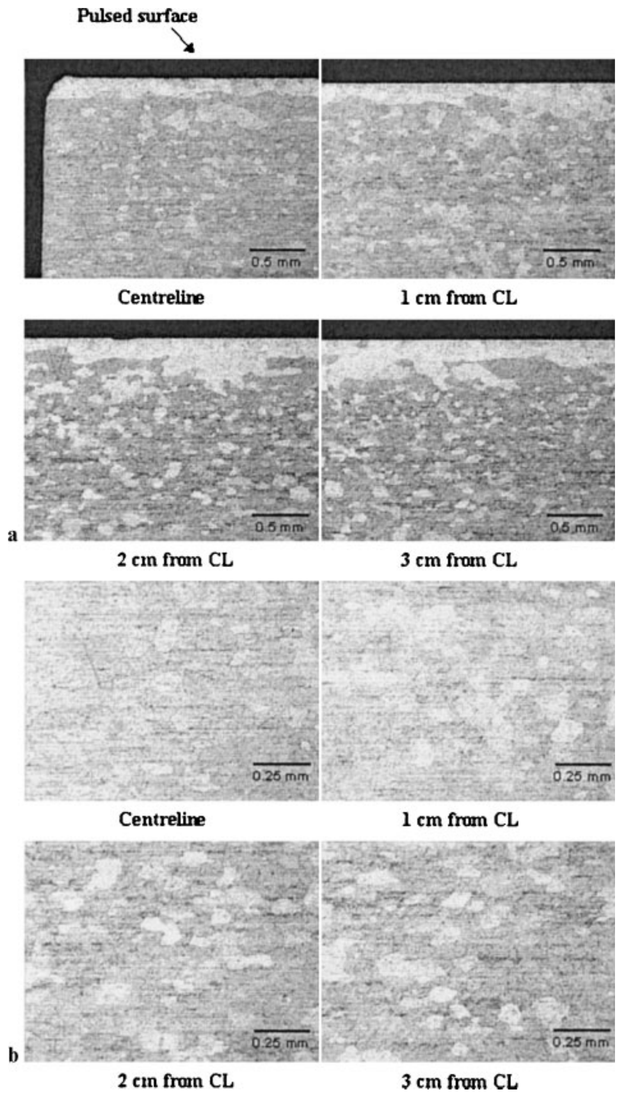

a near surface of sample from directly under centreline of lamp to 3 cm from centreline of lamp; *b* near centreline of sample for same locations

14 *Microstructure of 0·7 kW cm*$^{-2}$*, 8 s pulse aluminium samples*

place within the structure of the aluminium, as discussed by Grabowski.[5] The self-diffusion coefficient is given from the Einstein relation and an Arrhenius form

$$D(T)=D_0 \exp(-E_A/kT) \quad (4)$$

where E_A is the activation energy for the diffusion process, T is the temperature, and k is the Boltzmann constant.

An ideal temperature evolution for annealing would be such that the temperature is instantaneously increased to T_{ref}, held constant for time *EPT*, and then cooled instantaneously. At each location in the part, the annealing process will be characterised by a certain temperature evolution $T(t)$. The *EPT* would be determined such that the same amount of annealing would occur for the two schedules, i.e. the isothermal hold at T_{ref} and the real process, obtaining

$$\int_0^{EPT} D_0 \exp(-E_A/kT_{ref})\mathrm{d}t=\int_0^{t} D_0 \exp[-E_A/kT(t)]\mathrm{d}t \quad (5)$$

therefore, *EPT* is given by[6,7]

$$EPT=\int_0^{t} \exp[E_a(1/T-1/T_{ref})/k]\mathrm{d}t \quad (6)$$

where E_a is the migration energy, T is the process temperature at time t, T_{ref} is a reference temperature, and k is Boltzmann's constant. In this case, $E_a=0·75$ eV (Grabowski *et al.*[5]), $T_{ref}=400°C$ (673 K) and Boltzmann's constant is $8·617\times10^{-5}$ eV K^{-1}.

The same geometry as the aluminium samples was considered in the numerical simulations. Figure 15 shows the mesh applied to the geometry. Table 3

Table 3 Thermophysical properties considered in modelling of HDI softened aluminium plates

Thermophysical property	Value, cgs
Thermal conductivity, k	2·0e+7
Specific heat, c_p	9·0e+6
Density, ρ	2·7
Emissivity, ε	0·11

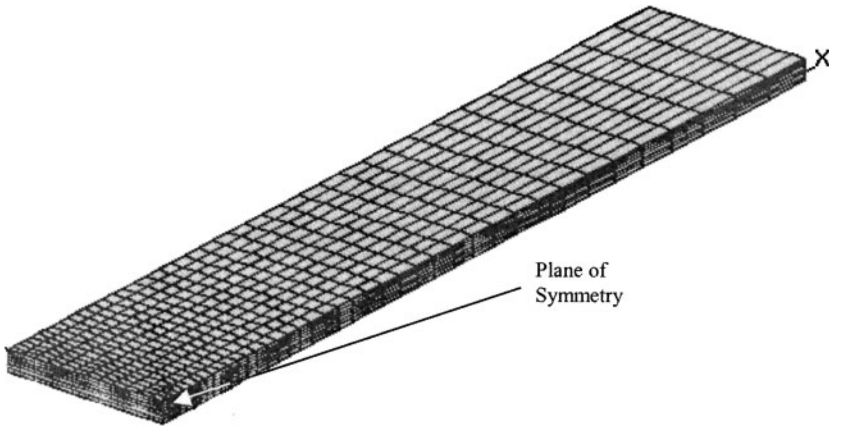

15 *Computational domain used for computer modelling of HDI softened aluminium plates*

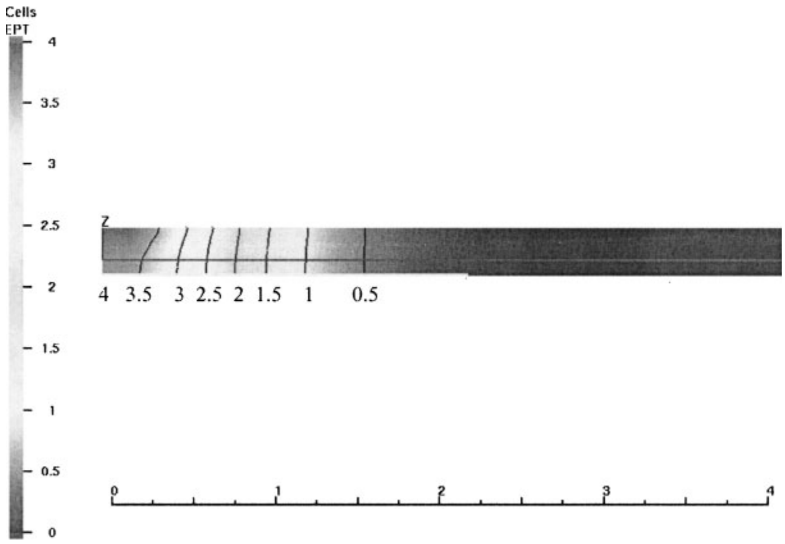

16 *Computational results of numeric simulation of 0·7 kW cm^{-2}, 8 s HDI pulse softening of aluminium (*EPT *parameter shown)*

shows the thermophysical properties considered in this simulation.

The computer simulations were conducted using the geometry of the aluminium samples and mesh from Fig. 15 with the thermophysical data from Table 3. The *EPT* parameter is shown in Fig. 16 for a simulation of the 0·7 kW cm^{-2}, 8 s pulse. According to Fig 7*b*, the heat affected zone for this sample begins 2 cm away from the centre of the lamp and reaches a maximum reduction in hardness at approximately 1 cm away from the centre of the lamp. Comparing these results with the *EPT* parameter, the maximum reduction in hardness is obtained when *EPT* is greater than 1·5 s and the heat affected zone begins when $EPT = 0{\cdot}5$ s. If $EPT \leqslant 0{\cdot}5$ or less, no significant reduction in hardness occurs. Based on the *EPT* threshold, the extent of the heat affected zone can now be predicted with confidence.

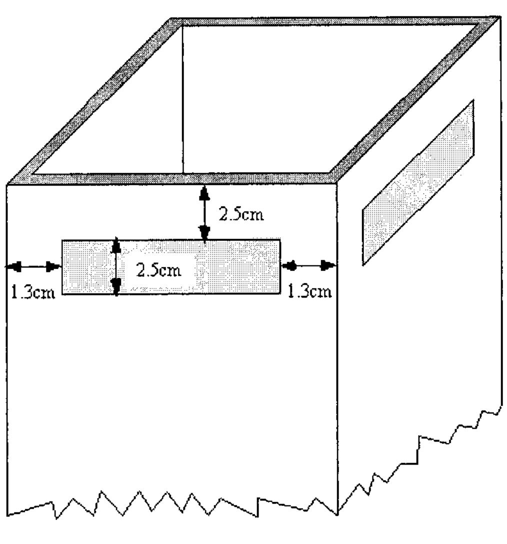

17 *Schematic of square tube showing shaded areas in which softening would allow for appropriate crash triggers*

MODELLING OF SQUARE TUBES

Applying the analysis to a tube structure will allow for the prediction of the heat affected zone using $EPT > 1{\cdot}5$ s as a criterion. Optimum processing parameters can then be determined such that the heat affected zone extends over a desired area. However, owing to the tube's higher thermal mass and the introduction of edges, much longer processing times may be required. Therefore, there is a critical need to model the heat flow during processing

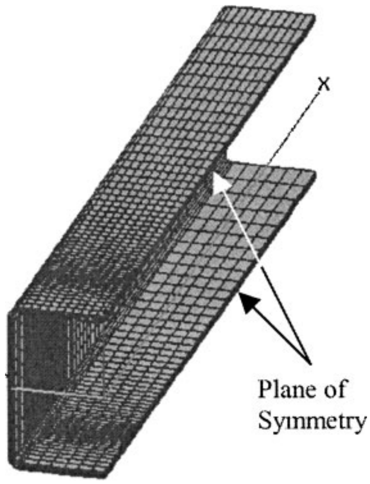

18 *Geometry and mesh applied for computer modelling of square aluminium tubes pulse HDI softened*

to obtain the appropriate reduction in hardness. Figure 17 shows the schematic of a square tube with the shaded areas that need to be softened. Numerical simulations were conducted using the thermophysical data in Table 3. The geometry and mesh are shown in Fig. 18.

A tube was pulsed on all sides with same parameters as one of the flat plates: 0·7 kW cm^{-2} for 8 s. The results of crush testing are shown in Fig. 19 for the as HDI processed tube and an as induction heated processed tube. Tubes that are induction heated show the appropriate crush behaviour, but the tube that was HDI pulsed does not. The induction heated tubes crush in a predictable manner which allows for the load to be distributed over a larger displacement.

Modelling of the aluminium tube exposed to an HDI pulse of 0·7 kW cm^{-2} for 8 s with the applied mesh and geometry shown in Fig 18 reveals why induction heating appears to have an advantage over HDI. Figure 20 shows the *EPT* parameter for the results of the computer model. It is evident that processing times must be longer than those of the flat plates. There is only a small area in which *EPT* was greater than 1·5 s, the lower threshold for a 50%

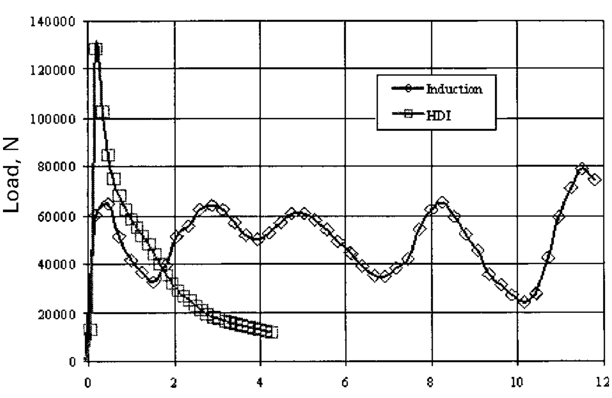

19 *Load versus displacement of crush tested aluminium tubes preferentially softened by HDI and induction heating*

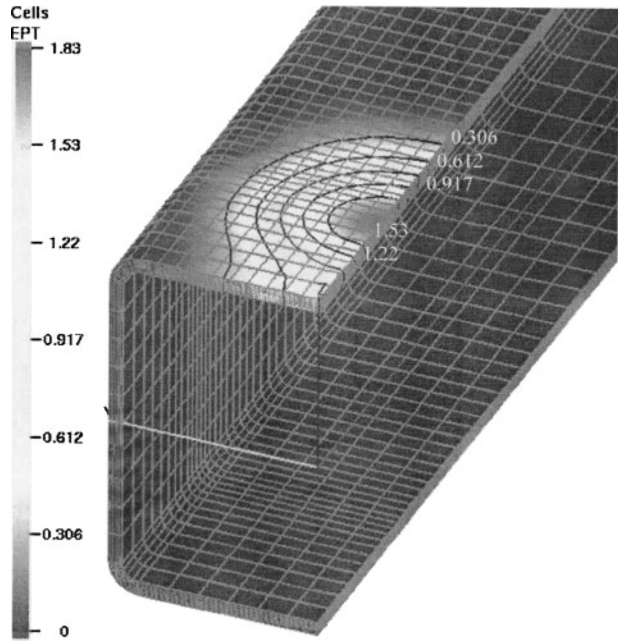

20 *EPT for 0·7 kW cm^{-2}, 8 s pulse*

reduction in hardness needed for the tubes to crush in a predictable and suitable manner. Longer processing times or higher process powers are necessary owing to the tube's higher thermal mass and the presence of edges on the tube. According to the schematic in Fig. 17, the heat affected zone, that is, where $EPT > 1{\cdot}5$ s, needs to be much larger. Further investigation needs to be performed using the computational tools now available. The prediction and execution of the appropriate HDI parameters for preferential softening of tubes is well within the capability of the computational tools available and within the capability of the plasma arc lamp processing facility at ORNL.

CONCLUSIONS

HDI plasma arc lamp processing has demonstrated potential as a viable alternative to current automotive production techniques. HDI would open the doors to widespread use of aluminium where previously only traditional materials could be used. Much success has been seen in the preferential softening of aluminium for use in automotive frame applications. Engineering the aluminium for the appropriate properties to tailor crash behaviours has been demonstrated. More work is required so that the application can be transitioned from flat plates to tubes. However, with the completion of a computer model that can predict thermal history, equivalent processing time and heat affected regions during HDI processing, this should be accomplished with little effort.

HDI is a robust processing tool which could easily be implemented in automotive assembly lines. At present, a processing facility which employs a plasma arc lamp mounted on a six axis robotic arm is functional at ORNL. The system is similar to a set-up that would be found on an assembly line and can process parts up to 35 cm wide and any length. Also, the long life and consistent operation of the lamp lends itself well to large scale processing. Furthermore, because of the radiant nature of the lamp, no contact is needed with materials being processed, and there are no open flames.

REFERENCES

1. M. SHIBATA, M. OONISHI, K. MAKINO and M. MIYAMOTO: *Mater. Jpn*, 1998, **37**, (6), 525–527.
2. D. M. CAMM and B. LOJEK: Proc. 2nd Int. Conf. on 'Rapid thermal', 1994, IEEE, Piscataway, NJ, USA.
3. C. A. BLUE, V. K. SIKKA, E. K. OHRINER, P. G. ENGLEMAN and D. C. HARPER: *JOM*, 2000, **52**, 8.
4. A. V. REDDY, D. B. KOTHE, C. BECKERMANN, R. C. FERRELL and K. L. LAM: Proc. 4th Int. Conf. on 'Solidification processing', University of Sheffield, UK, 1997, University of Sheffield.
5. S. GRABOWSKI, K. KADAU and P. ENTEL: *Phase Transitions*, 2002, **75**, (1–2), 265–272.
6. M. LEFRANCOIS and D. CAMM: Proc. 8th Int. Conf. on 'Advanced thermal processing of semiconductors, RTP2000', Gaithersburgh, MD, September 2000, IEEE, Piscataway, NJ, USA.
7. D. M. CAMM and M. LEFRANCOIS: Proc. 197th Meeting of the Electrochemical Society, Inc., Toronto, CA, May 2000, Electrochemical Society (ECS), Danvers, MA, USA.